**Research Article**

# Effect of IL-6R Inhibition with Tocilizumab on the Proteome of Peripheral Blood Mononuclear Cells from a Rheumatoid Arthritis Patient

**Michael Kruse Meyer[1,2], Marlene Andersen[1], Tue Bjerg Bennike[2], Svend Birkelund[2], Grethe Neumann Andersen[1] and Allan Stensballe[2,3]***

[1]Department of Rheumatology, Vendsyssel Teaching Hospital, Denmark, and Center for Clinical Science, Aalborg University, Denmark
[2]Department of Health Science and Technology, Aalborg University, Aalborg, Denmark
[3]Clinical Cancer Research Center, Aalborg University Hospital, Aalborg, Denmark.

## Abstract

**Objective:** The availability of biological disease-modifying anti-rheumatic drugs (bDMARDs) has increased during the last decade, and while focus has been on treating clinical symptoms, the associated changes in the immune system remains poorly understood. Several key immunological regulators, including Interleukin (IL)-6 are intimately associated with rheumatoid arthritis disease progression. In this *proof-of-concept* case study we assess the immunological changes in multiple important immune cell populations to treatment with the commonly applied bDMARD tocilizumab, a humanized monoclonal antibody against the IL-6 receptor.

**Methods:** Peripheral blood was obtained from one rheumatoid arthritis patient with poor response to conventional DMARD, before biological treatment and 4 months after. Peripheral blood mononuclear cells were extracted and separated into CD14+, CD4+, CD8+, CD19+, and CD56+ immune cells. Each cell-type was prepared through a discovery proteomics pipeline, and analyzed on a Q Exactive Plus mass spectrometer by gel-free shotgun proteomics.

**Results:** The patient responded well to tocilizumab monotherapy, and reached clinical remission without any observed side effects. A combined total of 4,343 proteins were identified at <1% false discovery rate, hereof 3,242 proteins qualified for label free quantification. We systematically evaluated the metabolic, inflammatory and signaling pathways of each immune cell type as a result of the IL-6R inhibition. The CD14+ cells were the most responsive to therapy, and proteins involved in the JAK/STAT and MAPK signaling pathways were less abundant.

**Conclusion:** Our data support that effective treatment of rheumatoid arthritis with tocilizumab causes decrease in the JAK/STAT and modulation of the MAPK signaling pathways, increases glucose metabolism, and reduces stress responses.

**Keywords:** Biomarker; Biobank; Mass spectrometry; Proteomics; Citrullination; Rheumatoid arthritis

**Abbreviations:** ASCs: Adipose-Derived Mesenchymal Stem Cells; BMSCs: Bone Marrow-Derived Mesenchymal Stem Cells; CM: Conditioned Media; DPSCs: Dental Pulp-Derived Mesenchymal Stem Cells; IPA: Ingenuity Pathway Analysis; MSCs: Mesenchymal Stem Cells

## Introduction

Rheumatoid arthritis (RA) is a systemic inflammatory joint disease, causing erosion of the joints and ultimately invalidity. RA is diagnosed through symptom evaluation of tender joints, swollen joints, and synovial hyperplasia with accompanying synovitis. The disease is thought to progress through an autoimmune phase, which begins with the break of tolerance to self-antigens, i.e. autoantigens. This leads to subclinical inflammation, succeeded by clinical inflammation, at which point the disease is often diagnosed [1]. Anti-citrullinated protein antibodies (ACPAs) are an early characteristic in the development of the majority of RA patients (up to 70%), and the presence of ACPAs is used to further establish the RA diagnose. Citrullination is a normally occurring protein modification of arginine, which *in vivo* is catalyzed by the peptidylarginine deiminase (PAD) family of enzymes [2,3].

Clinical diagnosis of RA is often not established until a patient has developed advanced autoimmunity. Therefore, the treatment with disease-modifying anti-rheumatic drugs (DMARDs) must be intensive to avoid further irreversible joint damage. Upon failure with conventional DMARDs, biological DMARDs (bDMARDs) are used to target specific pro-inflammatory mediators. The bDMARDs

are humanized antibodies against receptors or polymeric receptor pharmaceuticals. The increasing assortment of bDMARDs and number of *in vivo* targets has enabled multiple intervention points in the immunological cascade. A relatively new bDMARD, tocilizumab, is a humanized recombinant monoclonal antibody against interleukin 6 receptor (IL-6R) that prevents binding and signal transduction from the natural ligand IL-6. Blocking of the IL-6 signaling pathway has a strong therapeutic effect in RA patients, without major systemic toxicity [4-6].

Elevation in plasma IL-6 levels precedes a rise in C-reactive protein (CRP) [7]. CRP is an often used surrogate biomarker for inflammatory activity, and has potential for diagnostic use for monitoring early RA disease activity [8]. IL-6 stimulates the hepatic release of acute phase reactants, which makes the CRP concentration a surrogate marker for tocilizumab efficacy [9]. IL-6 signals through the JAK/STAT signaling pathway. Interestingly, IL-6R is also found secreted in a soluble form,

and is able to exert trans signaling in all glycoprotein (gp)130 expressing tissues [10]). Tocilizumab adequately prevents binding and activation of IL-6R throughout a dosing interval, confirmed by sustained high levels of tocilizumab-bound IL-6R complexes [11]. The inhibition of this signaling pathway is, therefore, thought to dampen further the inflammatory response.

In this *proof-of-concept* study, we examined the effects of IL-6R inhibition treatment on biological molecular pathways in a 59 year old female patient diagnosed with RA. The patient had an inadequate response to DMARD, and it was decided to initiate treatment with tocilizumab. To assess the immunological post-treatment outcome we applied quantitative proteome analysis to evaluate changes in the proteome profile of different biological pathways in leukocyte cell populations, important to RA pathogenesis. The leukocytes were isolated by positive enrichment of CD14+, CD4+, CD8+, CD19+, and CD56+ cells. Here we report a proteomic research method to measure IL-6R inhibition before and after start of treatment in a RA patient.

## Methods

The project was approved by the ethical committee of Northern Jutland, Denmark (N-20120074), and the participant had given an informed written consent to participate in the study. At the beginning of the study, the patient had a high disease activity, a poor response to regular DMARD, and was eligible for treatment with bDMARDs in accordance with "The Danish Rheumatic Society" guidelines.

### Peripheral blood mononuclear cell isolation and separation

Peripheral blood was collected in a EDTA vacutainer and mixed 2:1 (20mL + 10mL) with RPMI-1640 (Sigma Aldrich, St. Louis, USA), and centrifuged at 800 g for 30 min at 22°C in Accuspin System-Histopaque-1077 tubes (Sigma-Aldrich, St. Louis, USA). The plasma was discarded and the monocyte layer and residual Histopaque-1077 was diluted to a total volume of 50 mL with RPMI-1640, and centrifuged at 800 g for 10 min at 4°C. The supernatant was discarded and the PBMCs were resuspended into a total volume of 20 mL RPMI-1640, centrifuged at 800 g for 10 min at 4°C. The supernatant was discarded, and the PBMCs were resuspended into a total volume of 1 mL and centrifuged at 800 g for 10 min at 4°C. The supernatant was discarded and the PBMCs were resuspended with 1 mL binding buffer (0.1% BSA, 2 mM EDTA in $Ca^{2+}$ and $Mg^{2+}$ free PBS) and mixed with dynabeads (Thermo Scientific, Waltham, USA), as described by the manufacturer. The samples were incubated for 30 min and CD14+, CD4+, CD8+, and CD19+ cells were extracted using corresponding conjugated dynabeads in subsequent order. CD56+ was extracted using CD56 primary antibodies, and Goat-anti-mouse dynabeads Thermo Scientific, Waltham, USA), as described by the manufacturer. Separated cells were washed twice in $Ca^{2+}$ and $Mg^{2+}$ free PBS, and lysed in 350 µL denaturation and solubilization buffer (5% sodium deoxycholate (SDC), 100 mM dithiothreitol, 10 mM tetraethylammonium bromide (TEAB)). The total sample extraction, separation, and preservation of live cells never exceeded 7 hours. The samples from before treatment was stored for 4.5 months at -80°C, and the samples after treatment was stored for two weeks at -80°C. Subsequently, all samples were prepared for proteome analysis simultaneously, and analysed by LC-MS back-to-back in a randomized order to reduce experimental bias.

### Proteomics – sample preparation

Separated cells were prepared for proteomics analysis using a modified filter-aided sample preparation protocol, essentially according to Bennike et al. [12], where 100 µg protein, measured on a NanoDrop 1000 (Thermo Scientific, Wilmington, DE, USA) was extracted from the cell lysates, and used for downstream processing. The cell lysates were transferred to YM-10kDa spin filter (Millipore) and centrifuged at 11.000 g for 15 min at 4°C. The proteins were reduced with 12 mM Tris (2-Carboxyethyl) phosphine in 5% sodium deoxycholate (SDC), 10 mM TEAB for 30 min. at 37°C, and alkylated with 40 mM iodoacetamide in 5% SDC, 10 mM TEAB for 20 min at 37°C in the dark. Samples were centrifuged at 11.000 g for 15 min at 4°C after each step. In preparation for digestion, the buffer was exchanged by addition of digestion buffer (0.5% SDC, 50 mM TEAB) and centrifuged for 15 min at 4°C. A 1:50 (w/w) trypsin to protein ratio was added to the spin-filter, diluted in 50 µL digestion buffer followed by overnight trypsin digestion. The peptides were retrieved with 50 mM TEAB buffer and a phase separation was performed in 3:1 (v/v) ethyl acetate:sample acidified by addition of formic acid (FA) to a final concentration of 0.5%. Total phase separation was achieved by 2 min agitation and centrifugation at 11.000 g for 2 min at 4°C. The aqueous phase was collected and dried in vacuum in preparation for resuspension in LC-solution (2% acetonitrile (ACN), 0.1% FA).

### Proteomics – mass spectrometry analysis

The injected peptide sample amounts per UPLC-MS analysis was normalized using absorbance at 280 nm measured on a NanoDrop 1000 (Thermo Scientific, Wilmington, DE, USA) which was calibrated with LC-solution. 5 µg total peptide was analyzed per UPLC-MS run, diluted with LC-solution to a total volume of 10 µL, and the samples were analyzed in a random order in triplicates. The acquisition of MS-data was obtained in one block during approximately one week. The triplicates were analyzed consecutively (i.e. not randomized), and followed by a quality control with BSA to ensure system performance, retention-time stability, and to minimize sample cross contamination between different samples.

The samples were analyzed using an UHPLC-nanoESI MS/MS setup with a Dionex RSLC nanopump (Dionex/Thermo Scientific, Waltham, USA). The system was coupled online with an emitter for nanospray ionization picotip 360-20-10 (New objective, Woburn, MA, USA) to a Q Exactive Plus mass spectrometer (Thermo Scientific, Waltham, USA). The peptide material was loaded onto a C18 reversed phase column (Dionex Acclaim PepMap RSLC C18, 2 µm, 100 Å, 75 µm × 2 cm) and separated using a C18 reversed phase column (Dionex Acclaim PepMap RSLC C18, 2 µm, 75 Å, 75 µm × 50 cm) kept at 40°C. The sample was eluted with a gradient of 96% solvent A (0.1% FA) and 4% solvent B (0.1% FA in ACN), which was increased to 8% solvent B on a 5 minutes ramp gradient and subsequently to 30% solvent B on a 225 minutes ramp gradient, at a constant flow rate of 300 nL/min. The mass spectrometer was operated in positive mode, selecting up to 12 precursor ions based on highest intensity for HCD fragmenting.

### Proteomics – data analysis

The raw data-files were searched using MaxQuant 1.5.1.2 against all reviewed *Homo sapiens* Uniprot proteins (November, 2014). Standard settings were employed with carbamidomethyl (C) as a static modification, and protein N-terminal acetylation, deamidation (NQ) and citrullination (R), and phosphorylation (STY) were included as variable modifications. All proteins and peptides are reported below a 1% false discovery rate (FDR) cutoff, to ensure only high-confidence protein identifications.

The results were processed using Perseus v1.5.0.31. Initially, all reverse database hits and proteins tagged as contaminants (i.e.

abundant plasma proteins) were removed from further analysis, and the data was log2-transformed. Two unique peptides or more were required for a protein identification and quantification to ensure high-quality quantification. The protein abundances were investigated triplicate-wise, by scatterplots of all protein quantifications to evaluate reproducibility. For the purpose of conducting principal component analysis (PCA), missing values were replaced by imputation with values from a normal distribution (width 0.3 and down shift 1.8), calculated separately for each cell type to simulate signals from low-abundant proteins. For the analysis we compared Day 0 samples vs. Day 4 months treatment samples [13]. Proteins with a statistically significant abundance change prior to and following treatment were identified for each cell type using two-sample t-tests. As several thousand t-tests were performed, the results were corrected for multiple hypothesis testing in Perseus using permutation based FDR with standard parameters (FDR=0.05, S0=1 and 250 randomizations) [12,14]. A volcano plot was generated with x-axis $\log_2$ (mean protein abundance differences), and y-axis $-\log_{10}$ (mean difference p-value). Based on the 5% permutation-based FDR a significance cutoff was included. A subset of the protein associations were analyzed into greater detail based on associated KEGG pathways, metabolic and signaling pathways and Gene ontology groups (Activation of immune response; Activation of innate immune, acute inflammatory response, acute-phase response). The mass spectrometry proteomics data have been deposited to the ProteomeXchange Consortium via the PRIDE partner repository with the dataset identifier PXD002686 [15,16].

## Results

### Clinical response to IL-6R inhibition

The patient was a 59 year old woman, diagnosed with RA according to American College of Rheumatism (ACR) / European League Against Rheumatism (EULAR) criteria, with a high disease activity measured DAS28 of 5.0 (reference below 2.4), as seen in Table 1. The patient was RF and ACPA positive, non-erosive and antinuclear antibody negative. Three different DMARDs (first methotrexate oral, then methotrexate subcutaneous then sulfasalazine combined with leflunomide), were applied with no improvement, before treatment with tocilizumab monotherapy was initiated. In the study period, the patient was additionally treated with alendronic acid for osteoporosis and small amounts of clobetazol propionate cream for pustulosis palmoplantaris. After 4 months of tocilizumab treatment, clinical remission was reached and the patient did not develop any side effects.
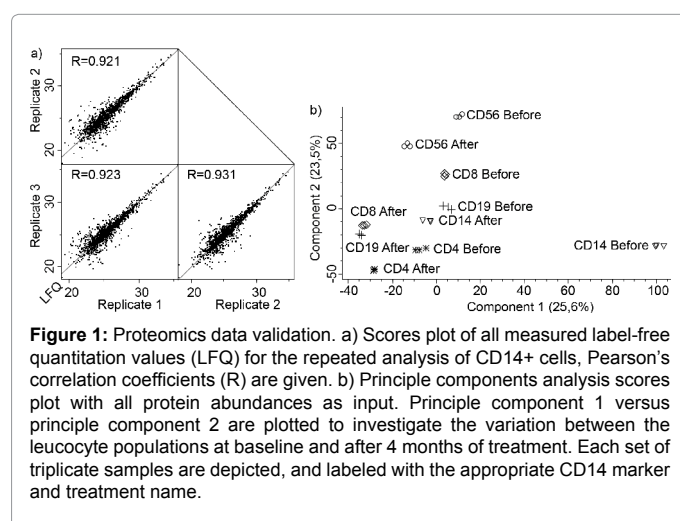
### Method validation for replica runs and cell isolation

Five cell populations were isolated before and after four months of tocilizumab treatment. Technical triplicates were run on the mass-spectrometer for each of the 10 isolated cell lines, giving at total of 30 MS runs. An unsupervised principal component analysis (PCA) based on overall proteome data was performed to evaluate replicate co-localization, isolation grouping, and treatment response, seen in Figure 1. All technical triplicates group together, confirming a high repeatability of the applied method. The PCA also provides insight into the response of treatment for each cell type. The CD14$^+$ cellular proteomes were overall the most changes as indicated by the distance on the scores plot of PC1 between the samples "CD14 before" versus "CD14 after treatment". Finally, the PCA indicates that each cell type can be uniquely identified from its proteome, and that the entire proteome changes after four months of treatment, likely as a response.

The CD14, CD4, CD8A, CD19 marker proteins were uniquely

| Parameter | Before treatment | After 4 months | Unit and Reference value |
|---|---|---|---|
| Date | 29-11-2013 | 12-03-2014 | DD-MM-YYYY |
| Age | 59 | | Years |
| Disease duration | 96 | | Months |
| CRP, | 8 | <2.9 | mg/L (<2.9) |
| Hemoglobin | 8,9 | 8,6 | mmol/L (7.3 - 9.5) |
| Leucocytes | 8,5 | 6,1 | x10^9 (3.5 - 10.0) |
| Neutrophils | 5,55 | 3,05 | x10^9/L (2.00 - 7.00) |
| Lymphocytes | 2,13 | 2,56 | x10^9/L (1.30 - 3.350) |
| Platelets | 196 | 148 | x10^9/L, (165-400) |
| IgM-REF, positive | 70 | | mM/L (<5) |
| ACPA, positive | >600 | | Unit/L (<10) |
| ANA | negative | | |
| Methotrexate | 0 | 0 | |
| Leflunomid | 0 | 0 | |
| Corticosteroids | None | None | |
| Prednisolone | 0 | 0 | (mg/day) |
| DAS28-CRP | 5.0 | 2.4 | |
| CDAI | 31.2 | 5.3 | |
| HAQ score | 0.625 | 1 | |
| VAS pain | 61 | 32 | |
| VAS fatigue | 62 | 32 | |
| VAS Global | 67 | 35 | |
| Doctors VAS | 45 | 8 | |
| Swollen join count 40 | 8 | 0 | |
| Tender join count 40 | 12 | 1 | |

**Table 1:** Clinical scores, and biochemistry values at baseline, and after treatment with tocilizumab. CRP=C-reactive protein, ACPA=anti citrullinated protein antibody, ANA=antinuclear antibodies, DAS28-CRP=disease activity score based on CRP and 28 joint count of swollen/tender joints, CDAI=Clinical Disease Activity Index, HAQ=Health Assessment Questionnaire, VAS=visual analogue scale.



**Figure 1:** Proteomics data validation. a) Scores plot of all measured label-free quantitation values (LFQ) for the repeated analysis of CD14+ cells, Pearson's correlation coefficients (R) are given. b) Principle components analysis scores plot with all protein abundances as input. Principle component 1 versus principle component 2 are plotted to investigate the variation between the leucocyte populations at baseline and after 4 months of treatment. Each set of triplicate samples are depicted, and labeled with the appropriate CD14 marker and treatment name.

detected in their corresponding cell population based on positive enrichment, giving validation to the purification method. In addition these proteins were non-significantly different in abundance between

before and after, which further validates loading control, and normalization.

## Proteomics data overview

The isolated leucocyte populations were analyzed in technical triplicates resulting in a combined total of 4,341 identified proteins at 1% FDR, hereof 3,242 qualifying for label free quantification (supplemental tables 1-5; ProteomeXchange). Proteins with a statistically significant change in abundance between each leucocyte fraction before and during tocilizumab treatment were identified by two-sided independent sample t-test, and can be seen in Figure 2. The number of proteins with a statistically significant change of abundance versus all proteins was distributed as follows: CD4$^+$ cells 136/2,563, CD8$^+$ cells 677/2,267, CD19$^+$ cells 479/2,193, and CD56$^+$ cells 245/2,104. Based on the number of protein abundance changes, the CD14$^+$, and CD8$^+$ cell types were the most responsive to IL-6R inhibition. Based on the result, the CD4$^+$ cells and CD56$^+$ cells were the least responsive to IL-6R inhibition on the proteome level. We mapped quantified proteins to their respective signaling, gene ontology or metabolic pathways, where proteins related to glucose, tricarboxylic acid (TCA) cycle, and pentose phosphate is given for each of the five cell types in Table 2. For easy comparison, we converted the log2 transformed abundance changes to percentage, relative to time point Day 0.

## Acute phase and Treatment specific protein abundance changes

The proteomic data was further investigated with a focus on the treatment with IL-6R inhibition by tocilizumab and investigation of proteins associated to relevant biological processes if inflammation (activation of immune response; activation of innate immune; acute inflammatory response; acute-phase response). Proteins with a statistically significant abundance change known to be associated to

immune system activation and acute phase responses are presented in Table 3 and the complete list of differentiating proteins for each cell type is provided in supplemental tables 1-5.

An interesting discovery was that several Protein S100 family known to be involved in regulation of many cellular processes including inflammation demonstrated similar abundance changes throughout the different cell populations (Tables 1 and Supplemental table 1-5). Protein S100-A9 was less abundant during treatment in CD14$^+$, CD8$^+$, CD19$^+$, and CD56$^+$ to 9%, 9%, 41%, and 41%, respectively. On the other hand Protein S100-A10 was increased in abundance during treatment in CD14$^+$, CD8$^+$, and CD56$^+$ cells to 754%, 209%, and 199%, respectively. Protein S100-A11 abundance was decreased in CD14$^+$, and CD4$^+$ cells to 5%, and 41%, respectively, while Protein S100-A6 abundance was decreased to 5% in CD14$^+$ cells. S100-A8 and S100-A9 can bind and constitute the calcium-binding protein complex calprotectin. Calprotectin is released by neutrophils under inflammatory conditions and has the capacity to induce apoptosis in various cells [17].

The CD14$^+$ cells before and after treatment were investigated in greater detail. The DNA-dependent protein kinase catalytic subunit was found with 5,501% abundance (55-fold). This protein has been linked to methotrexate treatment in cell culture experiments, which this patient did not receive at during the sample period. Additionally, tyrosine-protein kinase csk (CSK) (4,831%, 48-fold), tyrosine-protein kinase lyn (LYN) (4,217%; 42-fold), ferritin family homolog 3 (FERMT3) (11,457%; 114-fold), and signal transducer and activator of transcription 1 (STAT1) (4,924%; 49-fold) were also among the top ten proteins measured with the highest overall abundance difference before and during treatment. CSK acts upstream from LYN, and both are important enzymes in intracellular inflammatory signaling pathways, e.g. TLR4, while FERMT3 is an activator of integrins in integrin-mediated platelet, and leucocyte adhesion. STAT1 is directly downstream from the IL-6R.

## Discussion

We have conducted the first in-depth immunoproteome analysis of different cell-types prior to and after treatment with tocilizumab, with the aim to identify differentiating signaling pathways of each cell type as a result of the treatment. Proteins displaying a statistically significant change in abundance were identified by two-sample t-tests with permutation-based FDR control. A single healthy control was omitted, because this experiment is based on paired samples, i.e. before and after treatment, which provides a large reduction in noise. Healthy controls are biologically very different, and therefore it is necessary to include several healthy controls, so that noise can be averaged out. Thus, the main result of the study is proteomic response profiles for each cell type, as a result of the treatment.

## Signaling through the JAK/STAT cascade

We investigated the known signal transduction pathways linked to IL-6 stimulation within the five immune cell types in order to gain a putative insight into the cytokine/hormone environment that the cells interact with. The regulation of the JAK/STAT pathway was analyzed in each cell type to investigate the direct response to IL-6R inhibition. Overall, the CD14$^+$ cells seemed to be most responsive to IL-6R inhibition followed by the CD19 cells, based on the number of proteins with differentiating abundances. The need for specifically targeting the classical IL-6R versus soluble-IL-6R has recently been discussed, because studies have shown that IL-6R expression in CD4$^+$ cells recovered from sites of disease (e.g. synovial fluid) lack expression
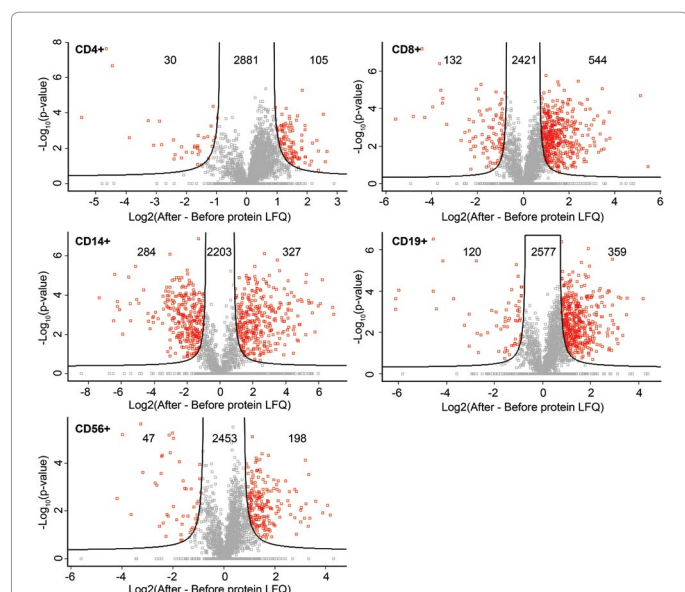


**Figure 2:** Each dot represent a quantified protein, and the significantly more abundant proteins have been highlighted in red. Positive differences indicates that the given protein is more abundant after treatment, and vice versa. The number of statistically more and less abundant proteins, as well as non-statistically significantly proteins is labelled on the figure. E.g. for CD14+, 327 proteins were significantly more abundant following 4 months of treatment, 284 proteins were signifantly less abundant, and 2203 proteins were not measured with a significant abundance change.

| Protein name | Accession number | Cell type and percentage abundance difference 0 vs 4 months (* Significant) | | | | |
|---|---|---|---|---|---|---|
| **Glycolysis** | | CD14+ | CD4+ | CD8+ | CD19+ | CD56+ |
| Phosphoglucomutase 1 | P36871 | **329.4% *** | 118.4% | 72.3% | 156.9% | 93.8% |
| Phosphoglucomutase 2 | Q96G03 | 1796.4% | 134.4% | **175.5% *** | 114.9% | 103.4% |
| Glucose-6-phosphate isomerase | P06744 | **864.5% *** | 91.4% | 104.9% | **252.6% *** | 122.2% |
| Hexokinase 1 | P19367-4 | **1946.9% *** | 144.3% | 132.7% | **192.9% *** | 114.2% |
| Hexokinase 3 | P52790 | **5310.6% *** | | | | 57.3% |
| Phosphofructoknase Type C | Q01813 | **645.7% *** | 165.4% | 113.9% | 152.9% | 120.3% |
| Fructose-1,6-bisphosphatase 1 | P09467 | **485.5% *** | 162.8% | 174.8% | **20.8% *** | **21.0% *** |
| Triose phosphate isomerase | P60174-1 | 171.0% | 105.5% | 146.4% | 120.5% | 122.9% |
| Glyceraldehyde 3-phosphate dehydrogenase | P04406 | 89.5% | 99.9% | 95.4% | 112.6% | 90.1% |
| Phosphoglycerate kinase | P00558 | 167.0% | 123.0% | 132.5% | 100.0% | 123.7% |
| Phosphoglycerate mutase | P18669 | 39.9% | 119.3% | 114.0% | 95.7% | 105.3% |
| Enolase | P06733 | 100.2% | 93.3% | 88.8% | 119.3% | -0,08 |
| Pyruvate kinase | P14618 | **341.2% *** | 133.6% | 122.7% | 144.0% | 112.3% |
| Phosphoenolpyruvate carboxykinase, mitochondrial | Q16822 | **516.1% *** | 103.8% | **472.1% *** | **22.0% *** | 119.6% |
| Alcohol dehydrogenase (class 3) | P11766 | **443,5% *** | 160.7% | **248.1%*** | **284.7%*** | 182.4% |
| alcohol dehydrogenase (NADP+) | P14550 | **726.1% *** | 148.9% | **276.2% *** | 77.8% | 109.5% |
| L-lactate dehydrogenase A chain | P00338 | **664.4% *** | 98.8% | 93.8% | 158.6% | 109.0% |
| L-lactate dehydrogenase B chain | P07195 | **231.0% *** | 126.1% | **57.8% *** | **176.5% *** | 136.6% |
| Pyruvate dehydrogenase | P11177-2 | **915.2% *** | 185.4% | **125.6%** | **71.5%** | **106.8%** |
| Aldehyde dehydrogenase, | P05091 | **684.1% *** | | | | |
| **TCA Cycle** | | | | | | |
| ATP-citrate synthase | P53396-2 | **1451.1% *** | 116.6% | **195.5% *** | 85.2% | 86.7% |
| Aconitate hydratase | Q99798 | **1343.3% *** | 113.2% | **167,4% *** | 72.5% | 143.5% |
| Isocitrate dehydrogenase [NADP] cytoplasmic | O75874 | **404.7% *** | 81.9% | 110.8% | 114.5% | 98.6% |
| Isocitrate dehydrogenase [NADP], mitochondrial | P48735 | **238.4% *** | 88.0% | 105.8% | 160.1% | 133.3% |
| 2-oxoglutarate dehydrogenase | F5H801 | 150.8% | 146.3% | 163.4% | **417.4% *** | 105.3% |
| Dihydrolipoyl dehydrogenase | B4DT69 | 101.0% | 86.9% | 116.3% | **151.7%** | 112.6% |
| Succinyl CoA synthetase | Q96I99 | **679.5% *** | 130.5% | **177.7% *** | 77.0% | 122.8% |
| Succinate deydrogenase | D6RFM5 | **434.8% *** | 78.8% | **211.5% *** | 171.9% | 198.7% |
| Fumarate hydratase | P07954-2 | **1636.1% *** | 156.4% | 155.8% | 81.9% | 107.0% |
| Malate dehydrogenase, cytoplasmic | P40925 | 61.5% | 79.8% | 145.3% | 75.9% | 158.1% |
| Malate hydrogenase, mitochondrial | P40926 | 92.7% | 83.4% | **254.9% *** | 162.3% | **187.7% *** |
| **Pentose Phosphate Pathway** | | | | | | |
| Glucose 6-phosphate dehydrogenase | P11413 | **1289.6% *** | 84.2% | 96.7% | 168.6% | 187.7% |
| 6-phosphogluconate dehydrogenase | B4DQJ8 | **360.0% *** | 103.6% | 99.1% | 130.1% | 109.2% |
| Ribose-5-phosphate isomerase | P49247 | 130.8% | -0,28 | **441.0% *** | | 120.8% |
| Transketolase | P29401 | **221.9% *** | 122.0% | 136.2% | 111.5% | 123.6% |
| Ribulose-phosphate 3-epimerase | Q96AT9 | 44.7% | 110.1% | 150.7% | 125.9% | 128.9% |
| Transaldolase | P37837 | 205.8% | 110.5% | **216.1% *** | 147.2% | 111.3% |
| fructose-1,6-bisphosphatase 1 | P09467 | **485.5% *** | 162.8% | 174.8% | **20.8% *** | **21.0%*** |
| 6-phosphofructokinase Type C | Q01813 | **645.7% *** | 165.4% | 113.9% | 152.9% | 120.3% |
| 6-phosphogluconolactonase | O95336 | **205.4% *** | 116.1% | 119.6% | 100.8% | 118.3% |
| glucose-6-phosphate isomerase | P06744 | **864.5% *** | 91.4% | **216.1% *** | **252.6%*** | 122.2% |
| Glutathione peroxidase 1 | P07203 | **192.4% *** | 61.6% | 93.1% | 100.1% | 117.6% |
| phosphoglucomutase 1 | P36871 | **329.4% *** | 118.4% | 72.3% | 156.9% | 93.8% |
| phosphoglucomutase 2 | Q96G03 | 1796.4% | 134.4% | **175.5% *** | 114.9% | 103.4% |
| Ribose-phosphate pyrophosphokinase 1 | P60891 | 477,3% | 147.9% | **387.2%*** | 117.0% | 125.3% |
| Ribose-phosphate pyrophosphokinase 2 | P11908 | | 125.4% | | 102.8% | 64.2% |

**Table 2:** Proteins annotated to the metabolic pathways glucolysis, TCA cycle, and pentose phosphate. Enzyme information from www.uniprot.org, and www.nextprot.org. Percentage protein abundance change is given for each cell type. *: Statistically significant change in abundance.

of IL-6R, but are responsive to IL-6 trans-signaling [18,19]. Therefore it may not be surprising that the CD4+ T cells were unresponsive to tocilizumab treatment, because this drug binds IL-6R and inhibits cell-expressed IL-6R and soluble IL-6R, thus inhibiting IL-6 trans-signaling.

The JAK/STAT pathways acts by activating the kinases Jak1, Jak2, and Tyk2, which in turn phosphorylates STAT1, STAT3, and STAT5 [20,21]. Treatment of the patient resulted in STAT1 being more abundant in CD14+ cells during treatment, and STAT3 being more abundant in in

| Cell type. and protein name GOBP • Activation of immune response • Activation of innate immune response • Acute inflammatory response • Acute-phase response | Accession number | Percentage abundance difference: Day 0 vs. 4 months | p-value | Protein sequence length | # peptides | % sequence coverage |
|---|---|---|---|---|---|---|
| **CD4+** | | | | | | |
| **Fibronectin** | P02751-10 | 604.1% | 5.51E-02 | 2176 | 28 | 21.6 |
| **Tyrosine-protein kinase BTK** | Q06187 | 316.3% | 9.51E-03 | 659 | 15 | 34 |
| **Stimulator of interferon genes protein** | Q86WV6 | 304.7% | 1.48E-04 | 379 | 7 | 32.5 |
| **Regulator of cell cycle RGCC** | Q9H4X1-2 | 263.6% | 5.34E-03 | 117 | 7 | 63.2 |
| **Nuclear factor NF-kappa-B p100 subunit** | Q00653-4 | 248.4% | 1.40E-02 | 899 | 6 | 11.2 |
| **Ig gamma-1 chain C region** | P01857 | 45.0% | 4.19E-05 | 330 | 11 | 49.1 |
| **Ubiquitin-conjugating enzyme E2 D2** | D6RAW0 | 39.4% | 7.86E-03 | 72 | 2 | 40.3 |
| **Apoptosis-associated speck-like protein containing a CARD** | Q9ULZ3 | 36.8% | 1.46E-02 | 195 | 13 | 72.3 |
| **CD8+** | | | | | | |
| **1-phosphatidylinositol 4.5-bisphosphate phosphodiesterase gamma-2** | P16885 | 1837.8% | 3.23E-03 | 1265 | 21 | 24 |
| **Serine/threonine-protein kinase D2** | Q9BZL6 | 677.2% | 2.04E-02 | 878 | 6 | 12.1 |
| **Nck-associated protein 1-like** | P55160-2 | 495.7% | 9.22E-05 | 1077 | 10 | 13 |
| **Complement component 1 Q subcomponent-binding protein. mitochondrial** | Q07021 | 361.5% | 2.80E-02 | 282 | 7 | 34.8 |
| **Ubiquitin-40S ribosomal protein S27a** | P62979 | 358.0% | 5.41E-05 | 156 | 11 | 51.9 |
| **Tyrosine-protein kinase SYK** | P43405 | 351.6% | 4.52E-04 | 635 | 11 | 33.2 |
| **Tyrosine-protein kinase CSK** | P41240 | 305.4% | 2.63E-03 | 450 | 19 | 53.6 |
| **Fibronectin** | P02751-10 | 304.6% | 2.47E-03 | 2176 | 28 | 21.6 |
| **Phosphatidylinositol 3.4.5-trisphosphate 5-phosphatase 1** | Q92835-2 | 297.9% | 2.48E-03 | 1188 | 20 | 28.5 |
| **Gamma-interferon-inducible protein 16** | Q16666-3 | 289.4% | 7.34E-05 | 673 | 22 | 42.6 |
| **Phosphatidylinositol 4.5-bisphosphate 3-kinase catalytic subunit delta isoform** | O00329 | 269.0% | 6.56E-02 | 1044 | 10 | 13.3 |
| **Tyrosine-protein kinase BTK** | Q06187 | 260.4% | 1.38E-02 | 659 | 15 | 34 |
| **Tyrosine-protein phosphatase non-receptor type 6** | P29350 | 207.4% | 4.49E-05 | 595 | 19 | 41.3 |
| **Receptor-type tyrosine-protein phosphatase C** | P08575-2 | 188.0% | 3.70E-04 | 1143 | 48 | 43.4 |
| **Ig kappa chain C region** | P01834 | 184.7% | 3.87E-04 | 106 | 7 | 90.6 |
| **Protein FADD** | Q13158 | 46.7% | 1.07E-02 | 208 | 3 | 22.1 |
| **Lymphocyte cytosolic protein 2** | Q13094 | 42.6% | 1.11E-03 | 533 | 16 | 32.1 |
| **Complement C3** | P01024 | 41.2% | 2.26E-04 | 1663 | 17 | 15 |
| **Protein S100-A8** | P05109 | 39.6% | 6.97E-03 | 93 | 10 | 51.6 |
| **GRB2-related adapter protein 2** | O75791 | 38.0% | 9.48E-05 | 330 | 12 | 50 |
| **Protein S100-A4** | P26447 | 32.9% | 7.58E-06 | 101 | 9 | 49.5 |
| **Cytoplasmic protein NCK1** | P16333 | 26.5% | 1.14E-02 | 377 | 6 | 24.4 |
| **Tyrosine-protein kinase Lck** | P06239 | 23.5% | 2.50E-02 | 509 | 11 | 30.3 |
| **Protein S100-A9** | P06702 | 7.3% | 8.90E-05 | 114 | 16 | 98.2 |
| **CD14+** | | | | | | |
| **Tyrosine-protein phosphatase non-receptor type 6** | P29350 | 4976.8% | 3.11E-03 | 595 | 19 | 41.3 |
| **Tyrosine-protein kinase CSK** | P41240 | 4724.3% | 2.48E-04 | 450 | 19 | 53.6 |
| **Tyrosine-protein kinase Lyn** | P07948-2 | 4250.9% | 1.85E-04 | 491 | 18 | 42.8 |
| **1-phosphatidylinositol 4.5-bisphosphate phosphodiesterase gamma-2** | P16885 | 2929.6% | 5.69E-03 | 1265 | 21 | 24 |
| **Receptor-type tyrosine-protein phosphatase C** | P08575-2 | 947.5% | 1.25E-04 | 1143 | 48 | 43.4 |
| **Cathepsin B** | P07858 | 918.2% | 7.25E-04 | 339 | 6 | 20.9 |
| **Platelet glycoprotein 4** | D9IX66 | 693.6% | 2.85E-03 | 412 | 8 | 21.1 |
| **Complement component 1 Q subcomponent-binding protein. mitochondrial** | Q07021 | 385.9% | 4.34E-03 | 282 | 7 | 34.8 |
| **Cathepsin S** | P25774 | 261.0% | 2.50E-04 | 331 | 6 | 20.8 |

| | | | | | | |
|---|---|---|---|---|---|---|
| Ubiquitin-conjugating enzyme E2 D2 | D6RAW0 | 221.3% | 9.89E-03 | 72 | 2 | 40.3 |
| Stimulator of interferon genes protein | Q86WV6 | 220.0% | 4.10E-03 | 379 | 7 | 32.5 |
| Ubiquitin-conjugating enzyme E2 N | P61088 | 195.8% | 1.40E-03 | 152 | 9 | 51.3 |
| Apoptosis-associated speck-like protein containing a CARD | Q9ULZ3 | 39.4% | 4.22E-02 | 195 | 13 | 72.3 |
| Ig kappa chain C region | P01834 | 39.4% | 9.83E-03 | 106 | 7 | 90.6 |
| 60 kDa heat shock protein. mitochondrial | P10809 | 35.9% | 9.10E-05 | 573 | 57 | 79.4 |
| FYN-binding protein | O15117 | 31.0% | 3.98E-03 | 783 | 18 | 35.9 |
| Haptoglobin | P00738 | 25.5% | 1.29E-01 | 406 | 6 | 28.1 |
| Lymphocyte cytosolic protein 2 | Q13094 | 15.6% | 7.33E-05 | 533 | 16 | 32.1 |
| Vasodilator-stimulated phosphoprotein | P50552 | 14.4% | 2.73E-04 | 380 | 23 | 49.2 |
| Wiskott-Aldrich syndrome protein | P42768 | 13.1% | 2.34E-04 | 502 | 14 | 43.2 |
| Alpha-1-antitrypsin | P01009 | 12.2% | 4.95E-03 | 418 | 11 | 22.5 |
| CCAAT/enhancer-binding protein beta | P17676-2 | 6.3% | 1.27E-03 | 322 | 2 | 14.6 |
| **CD19+** | | | | | | |
| | | | | | | |
| Fibronectin | P02751-10 | 1638.7% | 1.04E-04 | 2176 | NaN | 21.6 |
| Integrin beta | A8MYE6 | 1283.8% | 3.03E-03 | 712 | NaN | 41.9 |
| Phosphatidylinositol 4.5-bisphosphate 3-kinase catalytic subunit delta isoform | O00329 | 654.1% | 3.22E-04 | 1044 | NaN | 13.3 |
| FYN-binding protein | O15117 | 431.6% | 1.32E-04 | 783 | NaN | 35.9 |
| Signal transducer and activator of transcription 3 | K7ENL3 | 407.4% | 8.44E-04 | 722 | NaN | 24.9 |
| Ribosomal protein S6 kinase alpha-3 | P51812 | 276.8% | 9.40E-04 | 740 | NaN | 25.8 |
| GRB2-related adapter protein 2 | O75791 | 259.9% | 8.57E-05 | 330 | NaN | 50 |
| Platelet factor 4 | P02776 | 258.0% | 2.13E-03 | 101 | 11 | 42.6 |
| Nck-associated protein 1-like | P55160-2 | 230.3% | 8.49E-03 | 1077 | NaN | 13 |
| Lymphocyte cytosolic protein 2 | Q13094 | 223.5% | 1.25E-02 | 533 | NaN | 32.1 |
| Wiskott-Aldrich syndrome protein | P42768 | 209.7% | 5.62E-03 | 502 | NaN | 43.2 |
| Receptor-type tyrosine-protein phosphatase C | P08575-2 | 195.4% | 3.57E-06 | 1143 | NaN | 43.4 |
| Ig gamma-1 chain C region | P01857 | 194.5% | 6.81E-04 | 330 | 11 | 49.1 |
| Nuclear factor of activated T-cells. cytoplasmic 2 | Q13469-3 | 184.2% | 4.13E-03 | 901 | NaN | 20.9 |
| Regulator of cell cycle RGCC | Q9H4X1-2 | 178.6% | 6.55E-02 | 117 | NaN | 63.2 |
| Protein canopy homolog 3 | Q9BT09 | 175.2% | 9.62E-04 | 278 | 10 | 24.1 |
| Tyrosine-protein phosphatase non-receptor type 6 | P29350 | 51.5% | 1.38E-03 | 595 | NaN | 41.3 |
| Tyrosine-protein kinase SYK | P43405 | 41.1% | 1.64E-02 | 635 | NaN | 33.2 |
| Mitogen-activated protein kinase 14 | Q16539 | 40.6% | 2.38E-03 | 360 | NaN | 38.6 |
| Myeloid cell nuclear differentiation antigen | P41218 | 36.5% | 1.55E-04 | 407 | NaN | 36.1 |
| HLA class II histocompatibility antigen. DP beta 1 chain | F5H135 | 20.6% | 8.45E-03 | 123 | NaN | 36.6 |
| TNFAIP3-interacting protein 1 | E7EMV7 | 20.5% | 3.61E-05 | 492 | NaN | 7.7 |
| 1-phosphatidylinositol 4.5-bisphosphate phosphodiesterase gamma-2 | P16885 | 20.0% | 2.82E-04 | 1265 | NaN | 24 |
| **CD56+** | | | | | | |
| Fibronectin | P02751-10 | 505.6% | 1.51E-03 | 2176 | 28 | 21.6 |
| Wiskott-Aldrich syndrome protein | P42768 | 231.6% | 2.05E-04 | 502 | 14 | 43.2 |
| Tyrosine-protein kinase ZAP-70 | P43403 | 192.7% | 3.39E-02 | 619 | 15 | 32.3 |
| Tyrosine-protein kinase Fyn | Q5R3A8 | 174.5% | 5.76E-03 | 485 | 7 | 15.9 |

**Table 3**: Proteins annotated to the gene ontology biological processes activation of immune response, activation of innate immune response, acute inflammatory response, acute-phase response derived from the annotaion by Peresus. Fold regulation is given for each cell type (in percentage) as well, protein accession number (Uniprot), p-value, number of unique peptides and protein sequence coverage.

CD8+ and CD19+ cells during treatment. In addition, STAT6 was more abundant in CD19+ cells during treatment. Growth factor receptor-bound protein 2, which is associated to JAK/STAT signaling, was more abundant in CD14+ cells, suggesting an increased activation of programmed cell death. Protein phosphatase 1A was more abundant in CD14+ cells, which potentially make these cells less responsive to anti-inflammatory TGF-β signaling, but also less responsive to pro-inflammatory TNF-α signaling. Furthermore, phosphatidylinositol 4,5-bisphosphate 3-kinase was more abundant in CD8+ cells during treatment, suggesting more activation of cytokine production, and

proliferation. Interestingly, Tyrosine-protein phosphatase non-receptor type 6 was more abundant in CD14+ cells during treatment suggesting an increased capacity to turn off cytokine signaling.

The JAK-STAT pathway is intimately connected to the MAPK signaling pathway, which is responsible for cell proliferation, and apoptosis. However, the majority of proteins were not found with a statistically significant abundance change. Protein associated to the major inflammatory pathway of NF-κB were more abundant in CD4+, and CD19+ cells during treatment, indicating an activation of the pathway. Protein Kinase A was more abundant in CD4+, CD8+, CD19+, and CD56+ during treatment suggesting an upregulation in G-protein coupled receptor signaling, which acts upstream from this kinase. Interestingly, MAPK signaling in CD19+ cells seemed to be affected with several MAPKKKK's, and MAPKKK's significantly more abundant during treatment, but simultaneously with several MAPK's being less abundant during treatment. It is difficult to deduce the tentative consequences of the MAPK signaling changes, but it appears that the immune system is being modulated as an effect of the IL-6R inhibition.

### Metabolism overview - Glycolysis

Glycolysis was especially interesting, because the initial steps in this metabolic pathway generates energy anaerobically. Inflammation is an energetically expensive process that may deprive the tissues of oxygen. Thus, patients with systemic inflammation may experience anemia, and resulting fatigue [22]. Inflammation-induced high levels of IL-6 contribute to anemia through the induction of hepcidin synthesis with lowering of transmembrane iron transport, and circulating iron levels [23]. Thus supposedly, if oxygen is limited, anaerobic glycolysis may be preferable to some extent to generate the energy needed for cell homeostasis. Hence, during IL-6R inhibition, increased iron availability and thereby erythropoiesis will supply tissues with oxygen and reduce the need for anaerobically produced energy through glycolysis. In addition to glycolysis, we covered the TCA cycle to follow the flow of energy rich molecules, and pentose phosphate to analyze cellular protection against inflammatory induced reactive free radical species. The key enzymes in these metabolic pathways are tabulated in Table 3 and further documented in Supplement Table 6.

The CD14+ cells were the most responsive to the treatment as determined by the number of proteins with different abundance before and during treatment. We therefore focused our data-analysis on these cells. Key enzymes within the glycolysis pathway were found with increased abundance in the CD14+ in response to IL-6R inhibition. Six out of 11 enzymes in glycolysis were statistically more abundant, and additional 3 enzymes were less abundant (though not significant). In addition, the enzyme phosphoenolpyruvate carboxykinase was more abundant in the CD14+ cells, suggesting that more oxaloacetate is converted downstream to pyruvate. Within the glycolysis pathway hexokinase, and pyruvate kinase are especially important. When the amount of metabolites flowing into glycolysis decreases, the amount of metabolites flowing out from this process likewise decreases. When the energy charge is high, the activity of pyruvate dehydrogenase goes down. Interestingly, the abundance of pyruvate dehydrogenase was increased in the CD14+, CD8+, CD19+, and CD56+ cells during IL-6R inhibition. Considering the energy-need, it seems that the higher abundance of phosphoenolpyruvate carboxykinase and L-lactate dehydrogenase A/B in CD14+ cells, as well as the increased abundance of pyruvate dehydrogenase, in CD14+, CD8+, CD19+, and CD56+ cells during treatment, suggest an increased enzymatic activity to convert lactate in pyruvate, and ethanol into acetate during treatment. Overall, it seems that more energy is being produced through glycolysis during treatment (which induces disease remission), indicating that the cells experience less environmental stress and inflammation.

### Metabolism overview - TCA

Downstream from glucose metabolism, several proteins involved in the TCA pathway were significantly more abundant in CD14+ cells during treatment. Eight out of nine key enzymes were found with a differentiating abundance, of which seven were significantly different, and one non-significantly. This further establishes, that the aerobic energy production of the CD14+ cells has increased as a result of the biological treatment. The increase in the abundance of these enzymes was less pronounced in the other cells types. Spite most of the involved enzymes were non-significantly more abundant across the cells types, enzymes with a statistically significant abundance increase were identified. For example, citrate synthase was significantly more abundant in CD14+, CD8+, and CD19+ cells during treatment, suggesting an increased capacity to produce citrate in these cells, and thus potential for increased ATP production.

### Metabolism overview – pentose phosphate pathway

Reactive oxidative species (ROS) are produced as part of the inflammatory response, and confer oxidative stress on the cells, which may lead to cell damage and death [24,25]. Thus the metabolic pathways associated to this response were analyzed, e.g. the pentose phosphate pathway, which protects cells in the body from reactive oxygen species. Three of the four enzymes, which generate reducing power through the generation two NADPH molecules, were more abundant in the CD14+ cells during treatment. The increased reducing power is likely connected to the increased oxidative protection against reactive oxidative bi-products that necessitates reducing power. Concurrently, the various enzymes responsible for interconversion of sugars were more abundant during treatment, e.g. transketolase, and transaldolase, indicating an increased flow of metabolites back into glycolysis.

Furthermore, Glutathione peroxidase 1, which is a scavenger of ROS was more abundant in the CD14+ cells during treatment, further indicating an increased protection from radical scavengers. On the other hand superoxide dismutase, and catalase were both significantly less abundant during treatment, which could be a sign of increased aerobic metabolism, and at least an indication that sufficiently large numbers of radical scavengers are present.

Glucose-6-phosphate dehydrogenase is also responsible for the production of NADPH, which is used by Glutathione peroxidase 1 to reduce free radicals. Indeed this protein was also significantly more abundant during treatment in CD14+ cells, which suggest a regulation in oxidative stress.

### Protein S100-family regulation

The Protein S100-family is important in immune regulation, and has overlapping importance in inflammatory bowel diseases [12]. It has previously been shown that responders to methotrexate have higher level of S100-A9 measured in PBMC's, and non-responders have less expression. Our study suggests that S100-A9 might also be applicable as a marker for response to IL-6R inhibitors. The presented approach has shown that it is possible to locate the specific immune cells responsible for S100-A9 being less abundant during treatment, and further studies will show if this is consistent in larger groups of patients.

Overall, treatment with tocilizumab causes changes in the JAK/STAT and MAPK signaling pathways, increased the glucose metabolism, reduced cellular stress responses, and further insight into the regulation of important biomarkers in this case study.

## Conclusion

In this study we evaluated different signaling- and metabolic pathways in a female RA patient prior to and during IL-6R inhibition treatment with tocilizumab. The patient was found to have good clinical response to the therapy. We investigated proteome changes in the leucocyte cell populations of CD14^{+}, CD4^{+}, CD8^{+}, CD19^{+}, and CD56^{+} cells. Overall, the CD14^{+} cells were the most responsive to the treatment based on number of proteins found with a differentiating abundance. Tocilizumab treatment resulted in changes in the JAK/STAT and modulation of the MAPK signaling pathways, increased the glucose metabolism, and reduced stress responses. The patient has been classified as a good responder to tocilizumab and the entire dataset has been compiled into our growing spectral library of patient responses. We are expanding the database with the aim to stratify responders and non-responders based on the blood samples.

## Author Contributions

The manuscript was written through contributions of all authors. MKM conceptualized the overall study. MKM and MA collected samples for the study. MKM wrote the draft version of the paper and revised it according to co-authors comments. MKM performed the sample preparation; AS performed MS analysis. MKM performed the bioinformatics analysis. SB, AS, TBB, and GA contributed to the data analysis and supervised the study. All authors have given approval to the final version of the manuscript.

## Notes

The authors declare no competing financial interest.

## Supporting Information

All MS-proteomics data has been made publically available via ProteomeXchange with the dataset identifier PXD002686.

## References

1. Holmdahl R, Malmström V, Burkhardt H (2014) Autoimmune priming, tissue attack and chronic inflammation-the three stages of rheumatoid arthritis. Eur J Immunol 44: 1593-1599.

2. Ytterberg AJ, Joshua V, Reynisdottir G, Tarasova NK, Rutishauser D, et al. (2015) Shared immunological targets in the lungs and joints of patients with rheumatoid arthritis: identification and validation. Ann Rheum Dis 74: 1772-1777.

3. Bennike T, Lauridsen KB, Olesen MK, Andersen V, Birkelund S, et al. (2013) Optimizing the Identification of Citrullinated Peptides by Mass Spectrometry: Utilizing the Inability of Trypsin to Cleave after Citrullinated Amino Acids. J Proteomics Bioinform 6: 288-295.

4. Maini RN, Taylor PC, Szechinski J, Pavelka K, Bröll J, et al. (2006) Double-blind randomized controlled clinical trial of the interleukin-6 receptor antagonist, tocilizumab, in European patients with rheumatoid arthritis who had an incomplete response to methotrexate. Arthritis Rheum 54: 2817-2829.

5. Kremer JM, Blanco R, Brzosko M, Burgos-Vargas R, Halland AM, et al. (2011) Tocilizumab inhibits structural joint damage in rheumatoid arthritis patients with inadequate responses to methotrexate: results from the double-blind treatment phase of a randomized placebo-controlled trial of tocilizumab safety and prevention of structu. Arthritis Rheum 63: 609-621.

6. Woodrick RS, Ruderman EM (2011) Safety of biologic therapy in rheumatoid arthritis. Nat Rev Rheumatol 7: 639-652.

7. Tsigos C, Papanicolaou DA, Defensor R, Mitsiadis CS, Kyrou I, et al. (1997) Dose effects of recombinant human interleukin-6 on pituitary hormone secretion and energy expenditure. Neuroendocrinology 66: 54-62.

8. Bennike T, Birkelund S, Stensballe A, Andersen V (2014) Biomarkers in inflammatory bowel diseases: current status and proteomics identification strategies. World J Gastroenterol 20: 3231-3244.

9. Rossi JF, Lu ZY, Jourdan M, Klein B4 (2015) Interleukin-6 as a therapeutic target. Clin Cancer Res 21: 1248-1257.

10. Rose-John S, Heinrich PC (1994) Soluble receptors for cytokines and growth factors: generation and biological function. Biochem J 300: 281-290.

11. Zhang X, Peck R (2011) Clinical pharmacology of tocilizumab for the treatment of patients with rheumatoid arthritis. Expert Rev Clin Pharmacol 4: 539-558.

12. Bennike TB, Carlsen TG, Ellingsen T, Bonderup OK, Glerup H, et al. (2015) Neutrophil Extracellular Traps in Ulcerative Colitis: A Proteome Analysis of Intestinal Biopsies. Inflamm Bowel Dis 21: 2052-2067.

13. Krzywinski M, Altman N (2014) Points of significance: Comparing samples-part I. Nat Methods 11: 215-216.

14. Sotoca AM, Roelofs-Hendriks J, Boeren S, van der Kraan PM, Vervoort J, et al. (2013) Comparative proteome approach demonstrates that platelet-derived growth factor C and D efficiently induce proliferation while maintaining multipotency of hMSCs. Exp Cell Res 319: 2649-2662.

15. VVizcaíno JA, Côté RG, Csordas A, Dianes JA, Fabregat A, et al. (2013) The PRoteomics IDEntifications (PRIDE) database and associated tools: status in 2013. Nucleic Acids Res 41: D1063-1069.

16. Vizcaíno JA, Deutsch EW, Wang R, Csordas A, Reisinger F, et al. (2014) ProteomeXchange provides globally coordinated proteomics data submission and dissemination. Nat Biotechnol 32: 223-226.

17. Nakatani Y, Yamazaki M, Chazin WJ, Yui S (2005) Regulation of S100A8/A9 (calprotectin) binding to tumor cells by zinc ion and its implication for apoptosis-inducing activity. Mediators Inflamm 2005: 280-292.

18. Briso EM, Dienz O, Rincon M (2008) Cutting edge: soluble IL-6R is produced by IL-6R ectodomain shedding in activated CD4 T cells. J Immunol 180: 7102-7106.

19. Nowell MA, Williams AS, Carty SA, Scheller J, Hayes AJ, et al. (2008) Therapeutic Targeting of IL-6 Trans Signaling Counteracts STAT3 Control of Experimental Inflammatory Arthritis. J Immunol 182: 613-622.

20. Heinrich PC, Behrmann I, Haan S, Hermanns HM, Müller-Newen G, et al. (2003) Principles of interleukin (IL)-6-type cytokine signalling and its regulation. Biochem J 374: 1-20.

21. Heinrich PC, Behrmann I, Müller-Newen G, Schaper F, Graeve L (1998) Interleukin-6-type cytokine signalling through the gp130/Jak/STAT pathway. Biochem J 334 : 297-314.

22. Ganz T (2003) Hepcidin, a key regulator of iron metabolism and mediator of anemia of inflammation. Blood 102: 783-788.

23. Hunter HN, Fulton DB, Ganz T, Vogel HJ (2002) The solution structure of human hepcidin, a peptide hormone with antimicrobial activity that is involved in iron uptake and hereditary hemochromatosis. J Biol Chem 277: 37597-37603.

24. Weiss G, Schett G (2013) Anaemia in inflammatory rheumatic diseases. Nat Rev Rheumatol 9: 205-215.

25. D'Autréaux B, Toledano MB (2007) ROS as signalling molecules: mechanisms that generate specificity in ROS homeostasis. Nat Rev Mol Cell Biol 8: 813-824.